Int J Earth Sci (Geol Rundsch) (2005) 94: 180–192
DOI 10.1007/s00531-005-0467-2

ORIGINAL PAPER

Harald Karg · Andrew Carter
Manfred R. Brix · Ralf Littke

Late- and post-Variscan cooling and exhumation history of the northern Rhenish massif and the southern Ruhr Basin: new constraints from fission-track analysis

Received: 8 March 2004 / Accepted: 11 December 2004 / Published online: 3 March 2005

Abstract Apatite fission-track analyses were carried out on outcrop and core samples from the Rhenish massif and the Carboniferous Ruhr Basin/Germany in order to study the late- and post-Variscan thermal and exhumation history. Apatite fission-track ages range from 291 ± 15 Ma (lower Permian) to 136 ± 7 Ma (lower Cretaceous) and mean track lengths vary between 11.6 μm and 13.9 μm, mostly displaying unimodal distributions with narrow standard deviations. All apatite fission-track ages are younger than the corresponding sample stratigraphic age, indicating substantial post-depositional annealing of the apatite fission-tracks. This agrees with results from maturity modelling, which indicates 3500–7000 m eroded Devonian and Carboniferous sedimentary cover. Numerical modelling of apatite fission-track data predicts onset of exhumation and cooling not earlier than 320 Ma in the Rhenish massif and 300 Ma in the Ruhr Basin, generally followed by late Carboniferous–Triassic cooling to below 50–60°C. Rapid late Variscan cooling was followed by moderate Mesozoic cooling rates of 0.1–0.2°C/Ma, converting into denudation rates of <1 mm/a (assuming a stable geothermal gradient of 30°C/km). Modelling results also give evidence for some late Triassic and early Jurassic heating and/or burial, which is supported by sedimentary rocks of the same age preserved at the rim of the lower Rhine Basin and in the subsurface of the Central and Northern Ruhr Basin. Cenozoic exhumation and cooling of the Rhenish massif is interpreted as an isostatic response to former erosion and major base-level fall caused by the subsidence in the lower Rhine Basin.

Keywords Apatite fission-track analysis · Rhenish massif · Ruhr Basin · Exhumation · Cooling history

H. Karg · R. Littke
Institute of Geology and Geochemistry of Petroleum and Coal,
RWTH Aachen University, Lochnerstr. 4-20,
52056 Aachen, Germany

Present address: H. Karg (✉)
Wintershall Energía S.A., Maipú 757, Piso 7,
C1006ACI Buenos Aires, Argentina
E-mail: harald.karg@wintershall.com
Tel.: +54-11-55542739
Fax: +54-11-55542702

A. Carter
School of Earth Sciences, University and Birkbeck College,
Gower Street, London, WC1E 6BT, UK

M. R. Brix
Institut für Geologie, Mineralogie und Geophysik,
Ruhr-Universität Bochum, 44780 Bochum, Germany

Introduction

The geology of Central Europe is characterised by Variscan consolidation and deformation of pre-Permian rocks. These formations crop out in several fold-and-thrust belts such as the Rhenish massif (Fig. 1), but are partly overlain by several hundred to several thousand metres of Permian and younger rocks, e.g. in the Ruhr Basin (Fig. 1) and further north in the Central European Basin System (e.g. Glennie 2001; Verweij et al. 2003). Thermal maturation of the Pre-Permian is generally high, i.e. the hard coal or even anthracite stage has been reached.

Over the last two decades, the late Palaeozoic and Mesozoic thermal history of the Variscan Orogenic Belt in Central Europe has been subject to intense geological investigation. Most of this work was based on the numerical simulation studies using vitrinite reflectance data collected from individual wells (Littke et al. 1994; Büker et al. 1996; Hertle and Littke et al. 2000) or pseudo-wells constructed from outcrop information (Oncken 1991; Karg 1998; Nöth et al. 2001, see explanation of concept therein). Some of the investigations included 2D modelling (Büker et al. 1996; Karg 1998). The results from these studies revealed that the moderate to high level of thermal maturity, i.e. coalification, is due to deep burial and a moderate heat flow. Calculated

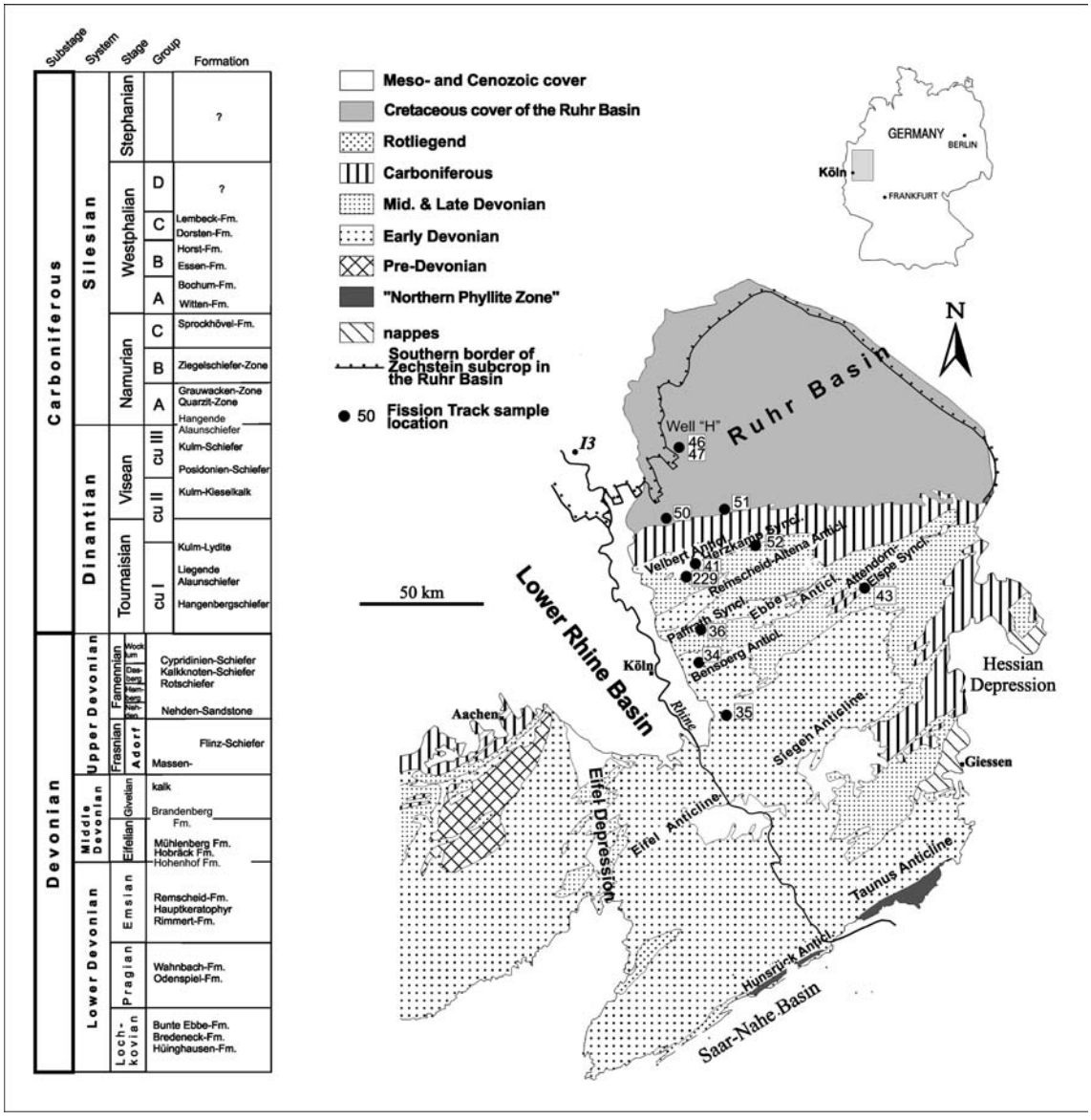

Fig. 1 Geologic map (modified after Walter, 1995) and stratigraphic chart of the study area with regional distribution of apatite and zircon fission-track samples

maximum burial data show a southward increase in depth of burial from about 2,000 m to more than 6,000 m in the Ruhr area/northern Rhenish massif (Büker et al. 1996; Littke et al. 2000). Deepest burial and maximum palaeotemperatures were reached during the latest Carboniferous or early Permian as indicated by a lower thermal maturation in the overlying late Permian (Zechstein) and Mesozoic deposits, i.e. a coalification "jump" can be found between the Variscan section and overlying rocks (Lommerzheim 1994; Büker et al. 1996). This history contrasts with that of the areas to the north in the Central European Basin, where maximum temperatures were reached during late Mesozoic or Cenozoic times. For the Ruhr Basin and the northern Rhenish massif, no systematic work to constrain the late- and post-Variscan temperature history has been published so far. Current reconstructions of late Variscan subsidence history, heat flow and eroded overburden in the Rhenohercynian, based on vitrinite reflectance data and thermal maturity modelling, show that up to 5,000 m of Devonian and Carboniferous sedimentary cover has been eroded during late Variscan orogenic phases (Büker 1996, Karg 1998, Littke et al. 2000). Borehole results from the Ruhr Basin indicate that this denudation phase had ceased before the Zechstein Sea flooded the previously formed erosional surface at ~257 Ma. In the Rhenish massif, there are no equivalent constraints from drilling so that the post-Variscan thermal and denudation history has remained poorly constrained. Some FT analyses on neighbouring Caledonian and Variscan basement highs by Vercoutere and van den Haute (1993) and Brix (2002) in the Brabant massif and in the Meuse Valley (Belgium), Glasmacher et al. (1998) in the Rhenish massif west of

the River Rhine and Büker (1996) in the eastern Rhenish massif and in the Ruhr Basin demonstrate that the FT method has potential to provide new insight into the post-Variscan evolution of the northern Rhenohercynian zone.

Other workers used K/Ar-dating of illite and sericite of Palaeozoic rocks of the Stavelot–Venn massif, to constrain deformation and cooling ages (Kramm et al. 1985; Tschernoster et al. 1995). They showed that a major deformation phase occurred around 300 Ma. Piqué et al. (1984) published K/Ar data on illites from the Rocroi massif (Belgium) and postulates a regional metamorphism to occur at about 330 Ma. Younger published information, on pressure and temperature conditions during the Variscan and partly the Caledonian deformation, obtained from mineral assemblages, illite crystallinity and vitrinite reflectance, was summarised by Fielitz and Mansy (1999).

The aim of this study is to try and fill the gap in understanding of the regional thermal history by employing fission-track analysis to constrain the late- and post-Variscan thermal and denudation history of the northern Rhenish massif, east of the River Rhine and the adjacent southern part of the Carboniferous Ruhr Basin. Fission-track analysis is ideally suited to this role and has been widely used to understand sedimentary basin evolution (e.g. Naeser et al. 1989 and references therein). The benefits of this method are best realised when the data are interpreted in conjunction with other basin analysis tools like numerical basin modelling. By integrating FT data with the results of basin modelling, we aim to establish a more complete reconstruction of regional thermal and exhumation histories for the Ruhr area/northern Rhenish massif region.

Geologic framework and regional setting

Tectonic processes during final stages of the Variscan orogeny caused a fundamental reorganisation of palaeogeography in Central Europe during late Palaeozoic times (e. g. McKerrow et al. 2000; Tait et al. 2000). The Variscan (Hercynian) fold-and-thrust belt extends from northwestern Spain, France, Britain and southwestern Ireland through central Germany into Poland in the east (Franke 2000).

At the front of the Variscan collisional fold-and-thrust belt, flexural bending of the stable continental crust, induced by the topographic load of the mountain chain itself caused the formation of the Subvariscan Foredeep as a classical foreland basin, providing accommodation space for a several kilometre thick clastic, and mostly coal-bearing late Carboniferous sedimentary succession. Ongoing and northward propagation of the orogenic front (Ahrendt et al. 1983) was the reason for major exhumation and erosion during late Carboniferous and Permian times. From the Carboniferous foreland basin in the north to the interior parts in the Saxothuringian and Moldanubian towards the south increasingly older sedimentary rocks with an increasing degree of thermal alteration and metamorphism crop out at the surface. Oncken et al. (1989, and various citations therein) published important work on the tectono–thermal evolution of the Rhenohercynian fold-and-thrust belt at a regional scale. It is the general understanding that, in the same sense as compression propagated northward, metamorphic ages become younger and the degree of thermal rock alteration diminishes. Until now, it was widely accepted that after this tectonism no renewal of subsidence occurred until present day.

Sampling and analytical methods

Fifteen rock samples were selected for apatite fission-track analysis. The majority of samples were collected from lower Devonian to upper Carboniferous outcrops in the Southern Ruhr Basin and the Northern Rhenish massif. Since igneous rocks are mostly absent from the study area, only sandstones were collected. The exception is sample 229, which was taken from a thin bentonite layer in lower Carboniferous strata from the Northern Rhenish massif. To optimise apatite yields unweathered immature medium grained sandstones were used for sampling. In addition, two samples are taken from cores of an exploration well in the Lippe Anticline (Western Ruhr Basin). A large vitrinite reflectance data set from a 2700-m thick column of coal-bearing upper Westfalian sedimentary rocks is available for this well, which allows better constraints to be placed on the sample thermal histories. The study area covers approximately 2500 km^2, which means that sample spacing is typically in the range of tens of kilometres. Although large, this is reasonable to identify regional trends in cooling history and by inference denudation. The sample stratigraphic and lithologic details are provided in Table 1.

The principal aim of this study is to use low-temperature thermochronology to constrain the Mesozoic and Tertiary thermal histories of the sampled lithologies. As above cited workers have shown, apatite fission-track analysis is a powerful tool to reconstruct cooling histories of rocks that have undergone thermal stress during orogenic processes. All apatite fission-track analyses were undertaken within the laboratories of the London Fission-track Research Group at University College London in collaboration with Ruhr-University Bochum.

For FT analysis, concentrates of apatite were obtained using conventional magnetic and heavy liquid separation techniques. Apatite mounting, polishing and etching followed standard procedures of the London Fission-track Research Group (apatite etching with 5N HNO_3 at 20°C for 20 s). Mounts were irradiated with muscovite external detectors and dosimeter glass CN-5 at the well-thermalised (Cd for Au > 400) thermal neutron facility of the Risø reactor, Denmark. Track

Table 1 Details of fission-track samples

Sample No.	Depth below surface (m)	Abs. Strat. Age (Ma)[a]	VR (%Ro)[b]	Present Temp. (°C)[c]	Sample location	Stratigraphy	*x*-coordinate (m)	*y*-coordinate (m)	Sample type	Lithology
34	0	390	1.2	10	Bensberg Anticline	Lower Emsian (lower Devonian)	2,585,450	5,647,000	Outcrop	Fine-grained sandstone
35	0	393	> 3.5[c]	10	Siegen Anticline	Upper Pragian (lower Devonian)	2,601,625	5,627,525	Outcrop	Fine-grained sandstone
36	0	~383	1.5	10	Paffrath Syncline	Eifelian (Middle Devonian)	2,583,740	5,656,250	Outcrop	Fine-grained sandstone
41	0	~322	1.4	10	Herzkamp Syncline	Namurian C (upper Carboniferous)	2,586,225	5,690,125	Outcrop	Medium-grained sandstone
43	0	~367	1.9	10	Elspe Syncline	Frasnian (upper Devonian)	3,443,870	5,678,120	Outcrop	Fine-grained sandstone
46	790	310	0.7	~30	Well "H", Lippe Syncline	Upper Westfalian C (upper Carboniferous)	–	–	Core sample	Medium-grained sandstone
47	1300	~312	0.9	~50	Well "H", Lippe Syncline	Upper Westfalian B (upper Carboniferous)	–	–	Core sample	Medium-grained sandstone
50	203	313	1.5	~18	Vestisch Anticline	Westfalian B (upper Carboniferous)	2,556,863	5,710,591	Mining subcrop, Zeche Osterfeld	Sandstone
51	27	314	2.0	10	Bochum Syncline	Westfalian A (upper Carboniferous)	25,070,400	5,694,200	Mining subcrop, Zeche Essen/Heidhsn.	Sandstone
52	0	383	2.5	10	Remscheid Anticline	Eifelian (Middle Devonian)	2,603,575	5,688,200	Outcrop	Fine- to medium-grained sandstone
229	0	~340	2.0–2.5[d]	10	Remscheid Anticline	Visé (lower Carboniferous)	2,583,657	5,684,555	Outcrop	Bentonite tuff

[a]The sample stratigraphic age was determined according to the standard stratigraphic charts of the Rhenohercynian and the Carboniferous of the Ruhr Basin (see also Fig. 1). The absolute stratigraphic ages were determined after Harland et al. (1989)
[b]Vitrinite reflectance data are published in Karg (1998)
[c]For the outcrop samples, the average mean annual surface temperature was taken, for borehole samples a geothermal gradient of 30°C/km was used to estimate the present-day temperature at the sampled depth
[d]Range of vitrinite reflectance values measured from nearby organic shales of similar stratigraphic age

densities were measured using a Zeiss Axioplan optical microscope at 1,250× magnification using dry objective. Central ages ($\pm 1\sigma$), according to Galbraith and Laslett (1993), were calibrated by the zeta method (Hurford and Green 1983), using a zeta factor of 339 ± 5, determined by multiple analyses of apatite standards following the recommendations of Hurford (1990).

A factor influencing the annealing behaviour of apatite is chemical composition. The annealing susceptibilities of F-apatite, Sr–F-apatite, and OH-apatite are similar and can be approximated by F-apatite data, whereas chlorapatites are significantly more resistant to annealing (Barabarand et al. 2003a, b; Ketcham et al. 1999). For this study, chemical composition was monitored using a combination of etch pit diameter (Donelick et al. 1999) and analysis by JEOL electron microprobe, using an accelerating voltage of 15 KV and a beam current of 29 nA, with a 20 μm defocused electron beam to avoid problems associated with apatite decomposition. In each sample, the majority of grains were found to have a restricted range in composition < 0.5 wt % Cl.

The abundance of vitrinite reflectance data combined with maturation modelling studies provides a useful addition to this study and serves to independently constrain parts of the sample thermal history. Those data are not discussed in detail, as they are described and interpreted by Büker (1996), Karg (1998), Littke et al. (2000) and Nöth et al. (2001).

Results and interpretation

Ideally, FT data suitable for quantitative FT analysis should have >15–20 single grain ages and >50–100 track-length measurements based on the horizontal confined fission-tracks. In this study, the quality of apatite data is generally good and can be modelled to constrain likely thermal histories. Most of the apatite FT central ages, as documented in Table 2, represent single grain age populations; only samples 52 and 47 from the Remscheid Anticline and the southern Ruhr Basin, respectively (Fig.1), show marginally significant dispersion in grain ages. The central ages range from 136 ± 7 Ma (lower Cretaceous) to 291 ± 15 Ma (Permian–Carboniferous boundary). All samples have central ages younger than sample depositional age (Fig. 2) indicating that post-depositional annealing has taken place to a more or lesser extent. The level of post-depositional annealing can be better investigated by looking at radial plots (Galbraith 1990), which show sample single grain ages relative to their sample depositional age (Fig. 3a). In five of the plots (samples 43, 46, 51, 52 and 229), the single grain age of the sample is displayed relative to its stratigraphic age, showing that the majority of apatite grains are significantly younger than depositional age and must therefore have experienced substantial post-depositional annealing. This observation is consistent with vitrinite reflectance data from organic-rich shales of the same stratigraphic age within the study area (Karg 1998; Littke et al. 2000) and FT data for the eastern Rhenish massif (Büker 1996).

Comparison between sample central age and mean track length in general shows no systematic relationship (Fig. 2), as would be expected from a region that experienced a uniform denudation history. The oldest central ages, between 291 ± 15 Ma and 238 ± 17 Ma (sample 46 from the Ruhr Basin and samples 41, 43 and 229, from the northern rim of the Rhenish massif). They record moderately long mean track lengths (MTL) consistent with long-term residence at moderately low tempera-

Table 2 Apatite fission-track analytical data

Sample	No. grains	Dosimeter tracks		Spontaneous tracks		Induced tracks		Age dispersion		Central Age $\pm 1\sigma$	Mean track length $\pm 1\sigma$	SD	No. tracks counted
		ρ_d	N_d	ρ_s	N_s	ρ_i	N_i	$P(\chi^2)$	RE %	(Ma)	(μm)	(μm)	
34	21	1.124	6,232	1.391	852	1.668	1,022	15	10.6	159 ± 9	13.90 ± 0.20	1.33	46
35	22	1.124	6,232	1.536	613	1.694	676	40	13.9	171 ± 11	13.07 ± 0.28	2.07	54
36	20	1.124	6,232	1.799	581	1.966	635	40	4.9	172 ± 10	12.91 ± 0.21	1.97	89
41	7	1.124	6,232	3.474	496	2.725	389	15	3.4	238 ± 17	12.43 ± 0.23	1.44	41
43	14	1.124	6,232	2.902	1,243	2.106	902	40	5.1	257 ± 13	12.54 ± 0.20	1.76	76
46	20	1.124	6,232	3.517	2,179	2.244	1,390	3	15.2	291 ± 15	11.98 ± 0.18	1.79	103
47	20	1.124	6,232	2.947	1,969	3.341	2,232	<1	19.4	167 ± 9	11.65 ± 0.17	1.82	122
50	16	1.203	6,667	2.351	909	3.478	1,345	32	8.2	136 ± 7	11.66 ± 0.23	2.33	103
51	13	1.203	6,667	4.021	875	3.768	820	77	1.7	214 ± 11	12.88 ± 0.18	1.76	99
52	9	1.203	6,667	2.337	434	2.164	402	2	20.8	216 ± 22	12.69 ± 0.26	2.20	72
229	25	1.205	6,679	1.696	1,093	1.213	782	44	6.6	280 ± 14	13.44 ± 0.14	1.57	122

(i) Track densities are ($\times 10^6$ tr cm^{-2}) numbers of tracks counted (n) shown in brackets
(ii) Analyses by external detector method using 0.5 for the $4\pi/2\pi$ geometry correction factor
(iii) Ages calculated using dosimeter glass CN-5 (apatite); analyst Carter ξCN5 $= 339 \pm 5$; ξCN2 $= 127 \pm 5$Calibrated by multiple analyses of IUGS apatite age standards (see Hurford 1990)
(iv) $P\chi^2$ is probability for obtaining χ^2 value for v degrees-of-freedom, where v = no. of crystals−1
(v) Central age is a modal age, weighted for different precisions of individual crystals (see Galbraith and Laslett, 1993)

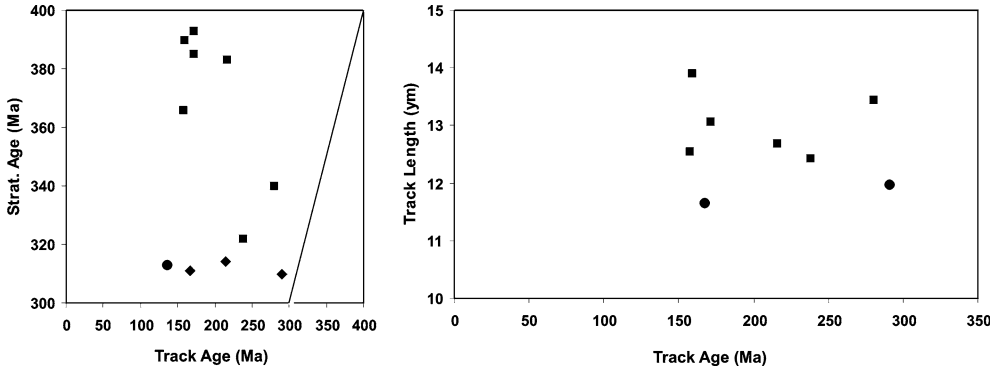

Fig. 2 *Left* Apatite fission-track central age versus sample stratigraphic age. All samples fall in the area left of the line, indicating that each sample has undergone significant annealing after deposition. *Right* Confined spontaneous track length versus fission-track age. Samples with the shortest confined tracks were all taken in wells from the Ruhr Basin, indicating most recent departure from the partial annealing zone (relative to the central age). *Squares* Samples from Rhenish massif; *filled circles* samples from Ruhr Basin

tures and by implication shallow crustal depths. Samples with ages between 216 ± 22 Ma and 159 ± 9 Ma (34, 35, 36, 51 and 52) has longer mean track lengths indicative of later cooling and residence also at shallow crustal depths. Borehole samples 47 and 50, from the central and the southern Ruhr Basin, respectively, have young FT ages (167 ± 9 Ma and 136 ± 7 Ma) and significantly shorter MTL's of 11.7 μm with a standard deviation of 2.3 μm.

To fully understand the significance of the data, they need to be considered in terms of sample location. Apatite length distributions for the entire study area are shown in Fig. 4 in relation to the geologic position of each sample. MTL vary between 11.6 μm and 13.9 μm and standard deviations between 1.3 μm and 2.3 μm, respectively (Table 2). Consequently, most

Fig. 3 Radial plots of apatite samples mentioned in the text. The position of each point on the *x*-scale records the uncertainty of individual age estimates, while each point has the same standard error on the *y*-scale (illustrated as $\pm 2\sigma$). The shaded segment on the plots represents the sample depositional age. For explanations, see text

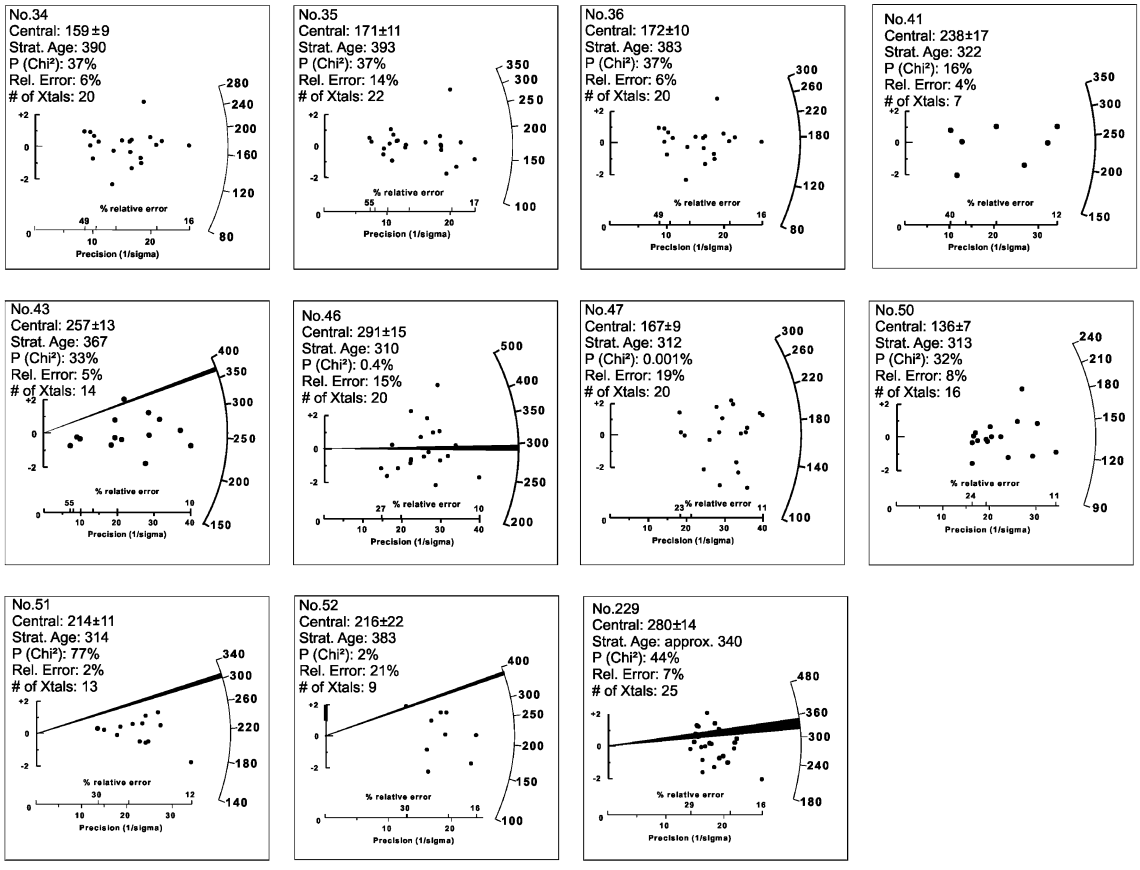

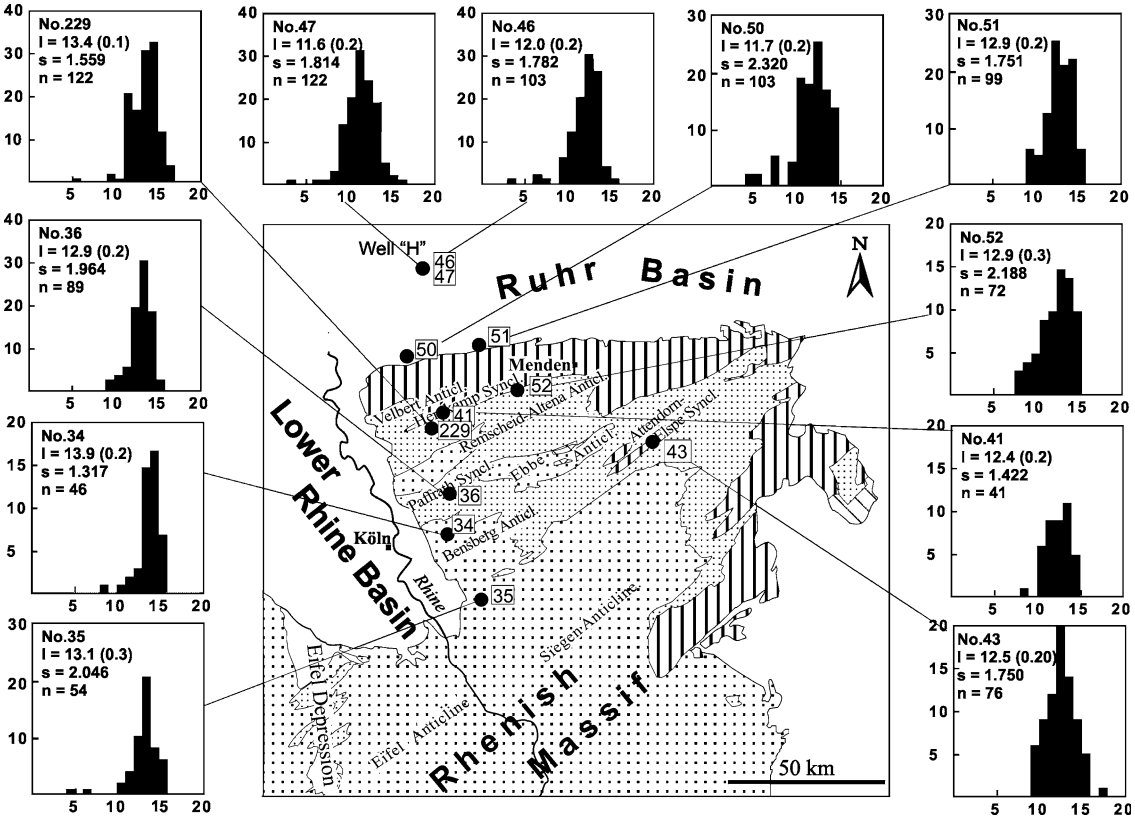

Fig. 4 Apatite fission-track results in their regional context. Here, frequency distributions of confined track lengths (spontaneous). The abscissa of the histograms represents the track length in μm; on the ordinate the percentage of individual tracks within the histogram classes are shown. *l* mean track length and relative error, *s* standard deviation, *n* number of counted tracks. For signatures in geologic map, see Fig. 1. Geologic map modified after Walter (1995)

measured tracks have experienced annealing, as they show significant shortening with respect to their initial length.

Thermal histories

Thermal history modelling is based on the mathematical models that describe track shortening at elevated temperatures for different time intervals. Those models allow prediction of fission-track age and length for any given thermal history (Green et al. 1989). Apatite composition, especially chlorine content, has a major influence on track annealing, hence, the importance of using an annealing model that is appropriate to the apatite sample composition. We used Laslett and Galbraith (1996) and compared our results against the multi-compositional annealing model of Ketcham et al. (1999). To recover sample thermal histories, we adopted the procedure developed by Gallagher (1995). This is a numerical search routine based on a data driven approach using Monte Carlo and genetic algorithm methods. Randomly generated thermal histories predict FT age and length parameters that are compared with measured data. The results are ranked and the best-fit selected using maximum likelihood. The time–temperature search space is unrestricted and therefore no search boxes are shown in Fig. 5. The only time-temperature restrictions used are sample depositional age, vitrinite reflectance data, unconformities, and present-day depth (either zero for surface samples or the respective borehole depth as reported for the sample was set). We assigned a present-day mean temperature of 10°C for surface samples. Because the modelling procedure is weighted towards the form of the track length distribution, modelling is only applied to those samples where the length distribution is adequately defined. For this reason, we did not model samples 34, 35 and 41. Examples of best-fit models are shown in Fig. 5. The shaded region on the plots shows represents the 2σ uncertainty extrapolated between error boxes. The dashed line on the plots shows the regions that are not constrained by the FT data.

Palaeozoic temperature history

Reconstruction of late Palaeozoic thermal histories is only possible for those samples which were not subjected to significant levels of heating during the Mesozoic and Tertiary. Sample 46 taken from well H in the Lippe Syncline, Ruhr Basin (Fig. 1) has a vitrinite reflectance value of 0.67%, which indicates only moderate levels of post-burial heating. The modelling results (Fig. 5) show

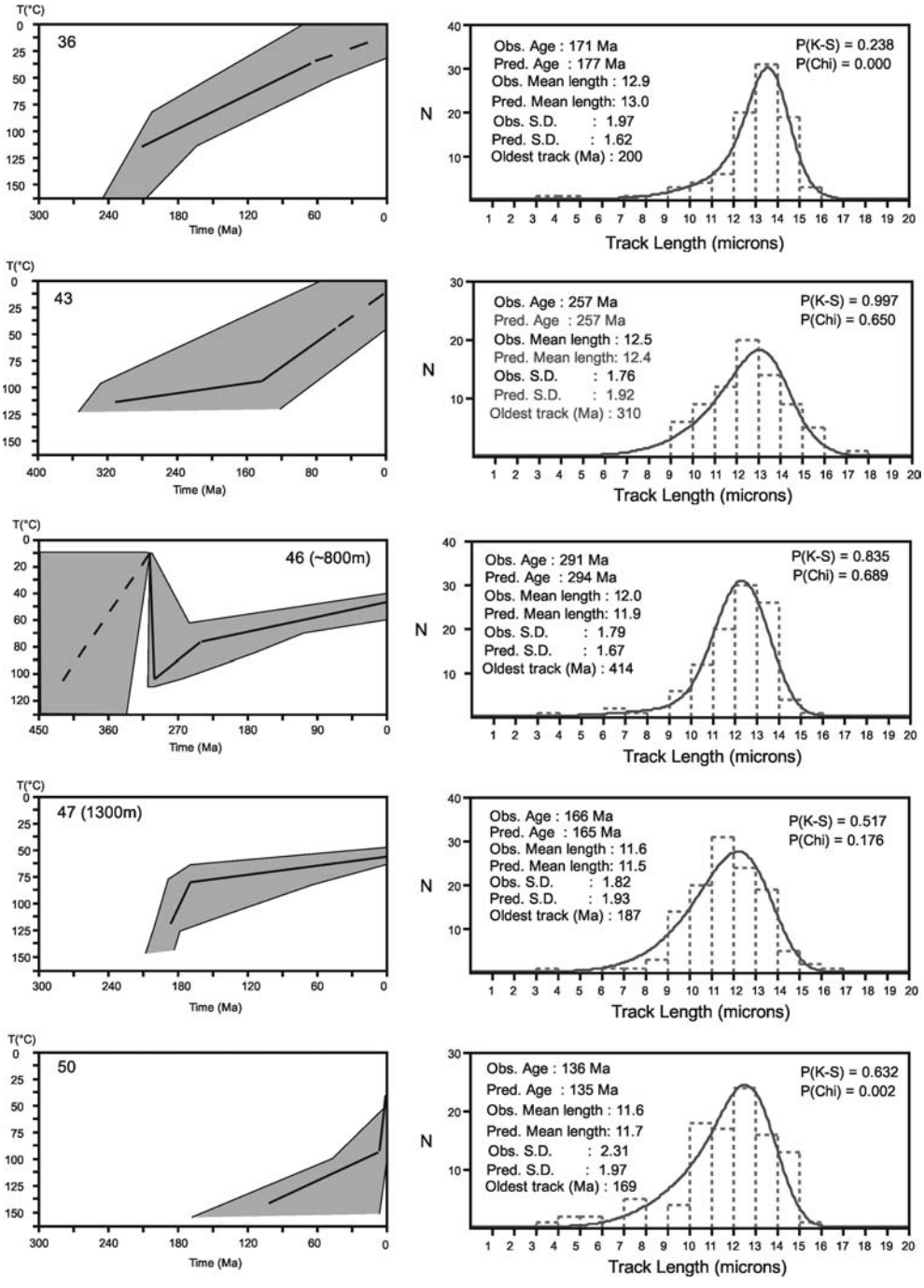

Fig. 5 Results of numerical simulation of fission-track thermal histories, using the approach of Gallagher (1995). Present-day mean temperatures, relative sample position to unconformities and thermal maturity data were taken as geological constraint. The *shaded region* on these plots represents the 2σ-uncertainty extrapolated between error boxes. The *dashed segments* of the lines in the plots indicate that these parts are not well constrained by the FT data

that sample 46 experienced peak temperatures soon after deposition, during the late Carboniferous or early Permian. Although this sample represents only partial thermal resetting, modelling results are reported, here, as they agree very well with results of 1D thermal basin modelling of this location. Karg (1998) calibrated the thermal history of this well using a detailed set of vitrinite reflectance data measured within the upper Carboniferous sequence. It could be shown that a thickness of 1400 m of Westfalian C and Westfalian D/Stefanian sediments had been removed during the Permian. Erosion must have occurred during the Early Permian, thus soon after sample deposition, as Zechstein sediments are preserved on top of the Westfalian C, forming an erosional unconformity. While the fission-track modelling results do not constrain maximum temperatures they do show that subsequently, cooling occurred at a moderately slow rate.

Another example providing insight into late Palaeozoic thermal history is the bentonite sample 229 from the northern rim of the Rhenish massif. The eruption age for this sample lies between 333 Ma and 350 Ma. The central age of 280 ± 14 Ma indicates post-depositional annealing, supported by vitrinite reflectance values

ranging between 2.0% and 2.5% measured in nearby stratigraphically equivalent organic-rich shales (Karg, 1998). However, few grains were detected that show ages equal to, or older than, the sample stratigraphic age. This suggests some minor partial resetting of older detrital apatite ages. Best-fit thermal histories for this sample indicate that peak post-depositional heating occurred prior to 300 Ma, followed by late Carboniferous–Triassic cooling to below 50–60°C. The subsequent Mesozoic thermal history of sample 229 is discussed in the next section.

Moving south, sample 43 from the Elspe Syncline in the eastern Rhenish massif shows a track length distribution similar to that of 229, but track lengths are more strongly reduced, implying a longer residence time within the partial annealing zone. The central age of the sample 43 is 257 ± 13 Ma and was obtained from 14 grains, belonging to a single population of grain ages. The central age, being significantly younger than the stratigraphic age of 367 Ma, and vitrinite reflectance values around 2% indicate total thermal resetting of the sample after deposition. Related maximum palaeotemperatures of 200°C for this sample were calculated through maturity modelling and were constrained by fluid inclusion measurements from the same sample (Karg 1998). The mean track length of 12.5 ± 0.2 μm has a unimodal distribution comprising 76 measurements. The observed track length distribution infers recent departure from the apatite partial annealing zone.

Modelling strategy of this sample involves time–temperature boxes with a maximum degree of uncertainty, as no t–T constraints were available, except the depositional age. The results of fission-track modelling provide a good fit to the measured data and the modelled mean t–T evolution path indicates that the sample reached maximum temperatures of >120°C prior to 320 Ma, followed by rapid cooling to temperatures of approximately 110°C, i.e. within, the deeper limit of the partial annealing zone, around 310 Ma. The sample then remained in a slowly cooling environment (cooling rate 0.1–0.2°C/Ma) within the partial annealing zone until the late Cretaceous/early Tertiary.

Sample 41 from the Southern Ruhr Basin exhibits poor apatite data results and therefore could not be modelled. However, the fission-track parameters are very similar to sample 43, making a similar thermal history style with rapid late Carboniferous cooling likely.

Mesozoic–Tertiary temperature history

In the Rhenish massif, few sedimentary deposits of post-Variscan times are available to reconstruct its post-Palaeozoic evolution. Mesozoic deposits are known from the subsurface of the lower Rhine Basin, the northwestern rim of the Rhenish massif and the northern Ruhr Basin, where undeformed sediments of Zechstein age rest on top of the erosional upper Carboniferous surface.

Looking at the fission-track age data, it can be seen that nearly every sample has a central age between 136 ± 7 Ma and 257 ± 13 Ma. These ages are interpreted as mixed ages as in most of the samples single grains with Palaeozoic ages are preserved. The observed spectrum of central ages thus reflects multiphase cooling since late Variscan with significant thermal resetting during Mesozoic times. Exceptions to this are samples 46 (291 ± 15 Ma) and 229 (280 ± 14 Ma), which clearly reflect early onset of cooling at late Carboniferous times. Both samples display incomplete thermal resetting as some grains with ages older than the sample stratigraphic age were observed. It is noteworthy that apatite pooled ages from samples of the Linksrheinisches Schiefergebirge (west of the river Rhine), published by Glasmacher and Zentilli (1998), display a very similar age spectrum between 130 ± 22 Ma and 239 ± 26 Ma.

Modelling the fission-track data, different Mesozoic thermal histories can be derived and partly related to the geographic sample origin.

The southernmost samples taken in the study area are lower and middle Devonian sandstones from the northern Siegen anticline (no. 35), the Bensberg anticline (no. 34) and the Paffrath syncline (no. 36). All three samples were collected in outcrops of lower to Middle Devonian rocks (Fig. 1) and have in common their proximity to a fault system, limiting the Tertiary lower Rhine Basin against the Rhenish massif and a complete thermal resetting of all provenance-related fission-tracks during Palaeozoic times, ascertained by the high rank of organic maturation, measured in associated pelitic rocks (see Table 1). Samples 34, 35 and 36 show a very similar track length and age distribution. However, only sample 36 was found to be suitable for modelling. Twenty individual grain ages were determined, each belonging to a single statistical population with a central age of 172 ± 10 Ma and with no major component of inherited tracks. Fission-track and vitrinite data of the sample clearly indicate effective thermal resetting. According to modelling, the sample remained at high palaeotemperatures (>120°C) at least until late Triassic times and stayed within the partial annealing zone until the upper Cretaceous. Considering the mean t–T path, cooling occurred at constant rates of about 0.1–0.2°C/Ma throughout the Mesozoic. For the late Tertiary, we can only estimate cooling rates by extrapolating to the present-day. This gives an average rate of ~0.5°C/Ma, slightly faster than in the Mesozoic. Although cooling has to be extrapolated, we cannot rule out the possibility that cooling in the Tertiary may have been faster for some samples. However, the borehole samples (46 and 47), which have remained in the partial annealing zone and were therefore sensitive to changes in Tertiary cooling, show no evidence that this has really taken place.

The results of the previously described samples fit very well into the modelling results for sample 229 (see the previous paragraphs) implicating that this sample underwent Triassic–Jurassic reheating to temperatures between 70°C and 80°C. For the time since the Jurassic, FT results require that the sample has remained at low temperatures (< 60°C).

The overall trend that the PAZ was not left prior to upper Cretaceous times is confirmed by most of the samples. Sample 43, from the Attendorn–Elspe Synline in the eastern part of the Rhenish massif, did not pass the 60°C isotherm before upper Cretaceous/early Tertiary times and modelling implies very low cooling rates between 0.1°C/Ma and 0.2°C/Ma throughout the Mesozoic. Suggesting continuous cooling during the early Tertiary, accelerated cooling rates, averaging at about 0.7°C/Ma, are inferred by extrapolation of the modelled *t–T* path to present-day temperatures. This sample also exhibits some grains older than the sample stratigraphic age.

Samples 50, 51 and 52 show similar thermal histories. However, sample 50 is similar to samples 34, 35 and 36, which indicate late cooling below 120°C. This sample (50) has experienced total resetting during upper Carboniferous subsidence. Best-fit between observed and modelled fission-track data was achieved under the assumption that the sample stayed within the PAZ throughout the entire Mesozoic period and was cooled below 60°C not before the late Tertiary. As *t–T* boxes for modelling have been kept with a maximum degree of uncertainty, even Tertiary reheating of the sample 50 cannot be excluded.

A very similar thermal history style is observed in samples 51 and 52 from the southern Ruhr Basin and the northern rim of the Rhenish massif, respectively. Both samples have been totally reset after deposition and the observed fission-track distributions can best be explained by assuming a long residence time within the PAZ covering the entire Mesozoic era. Following the modelled average *t–T* path, it can be concluded that sample 52 from the northern Rhenish massif entered the PAZ earlier than was the case in the adjacent Ruhr Basin (sample 51). Cooling below the 60°C isotherm occurred not before the early Tertiary; thus, Tertiary cooling might have been accelerated compared to Mesozoic cooling.

Discussion

Measured apatite fission-track central ages range from 291 ± 15 Ma (lower Permian) to 136 ± 7 Ma (lower Cretaceous, see Table 2). All apatite FT ages are younger than sample stratigraphic ages, indicating substantial post-depositional annealing. The distribution of apatite FT ages shows no relation to the geographic distribution of the samples. However, the stratigraphically oldest samples (lower and middle Devonian) taken from the central Rhenish massif, have notably younger ages (from 172 ± 10 Ma to 159 ± 9 Ma), while the stratigraphically youngest samples, from the central Ruhr Basin and the northern tip of the Rhenish massif (Figs. 1, 4), have the oldest fission-track ages of 291 ± 15 Ma (sample 46) and 280 ± 14 Ma (sample 229) (upper Westfalian and Visean stratigraphic ages, respectively). This indicates that the central Rhenish massif has experienced a greater amount of erosion than the central Ruhr Basin and the northern tip of the Rhenish massif. Mean confined track lengths range from 11.6 µm to 13.9 µm and typically show unimodal to slightly skewed distributions consistent with moderate to slow cooling through the apatite partial annealing zone. The qualitative evidence for significant post-depositional annealing based on the reduced central ages and MTL is consistent with a large vitrinite reflectance dataset from Devonian and Carboniferous organic-rich shales (Karg 1998; Nöth et al. 2001; Littke et al. 2000) that indicates erosion of a substantial thickness of Palaeozoic sedimentary rocks. Based on the vitrinite reflectance data presented by Karg (1998), it has been estimated that in the Northern Rhenish massif and the Ruhr Basin eroded thicknesses vary between 3,000–5,000 m and 1,500–3,500 m, respectively. These estimates of erosion require sedimentation to have lasted significantly longer than presumed by earlier workers (e.g. Patteisky et al. 1962). According to average late Carboniferous sedimentation rates, as published by Drozdzewski (1993) subsidence and deposition within major synclines could not have ended before the Early Stephanian. This is consistent with the FT thermal history results from sample 46 with a central age of 291 ± 15 Ma. As the erosional level is stratigraphically deeper in the Rhenish massif, where sedimentary rocks of Devonian age crop out, it is more difficult to estimate the duration of Palaeozoic sedimentation in this area. There is some evidence that sedimentation in the Rhenish massif only ended in the Namurian (or even later); otherwise erosion of ~3000 m of Palaeozoic sedimentary cover, as was deduced from calibration of organic maturation data (e.g. Nöth et al. 2001), is difficult to explain. This is supported by the modelled mean *t–T* path of sample 43, indicating entry into the partial annealing zone at ~ 320 Ma (upper to lower Namurian boundary) and thus marking the onset of Variscan denudation in this portion of the Rhenish massif. A temporal shift of the onset of Variscan denudation and cooling from Namurian times in the Rhenohercynian till late Westfalian or even Stefanian times in the Subvariscan Foreland areas is consistent with the widely accepted model of a northward propagating uplift and folding characterising final stages of Variscan orogeny in Middle Europe (compare Ahrendt et al. 1983; Oncken 1989; Drozdzewski 1993).

After rapid late Variscan cooling, FT thermal histories show that the samples generally remained in a slowly cooling environment (cooling rate 0.1–0.2°C/Ma), departing from the FT partial annealing zone in

the late Cretaceous/early Tertiary. Estimation of denudation rates based on the fission-track results is difficult since, given the regional polyphase geological history, a regionally and temporally constant geothermal gradient is unlikely. Heat flow would have changed during orogenic thickening of the Variscan crust during late Carboniferous and Permian times and during various phases of Mesozoic and Cenozoic mineralisation. However, late Variscan heat flow and the total thickness of eroded Palaeozoic sedimentary rocks are well constrained by coalification studies and previous maturity modelling. Estimates of palaeo-heat flow range between 45 mW/m^2 and 60 mW/m^2 for the Namurian and Wesphalian, with a tendency to decrease southwards (Littke et al. 2000; Nöth et al. 2001). Cooling rates derived from fission-track modelling are low to moderate and consequently denudation rates would have to have been low as well. Higher geothermal gradients would result in lower denudation rates. Assuming normal and constant geothermal gradients of 30°C/km since onset of sample cooling results in denudation rates for the Mesozoic of around 0.07 mm/a. These low erosion rates are similar to the fission-track results from Palaeozoic sandstones of the Rhenish massif west of the river Rhine (Glasmacher et al. 1998). In this study, estimated denudation rates for the Triassic and Cretaceous were 0.01 mm/a and 0.05 mm/a, respectively. Glasmacher et al. (1998) also inferred a "normal" and stable geothermal gradient since late Palaeozoic times.

Because the high level of burial related heating in the Rhenish massif has reset the apatite FT system, we cannot use samples from this region to constrain the time of maximum heating. Consequently, the question whether cooling continued without interruption or whether renewed subsidence and heating took place in some areas during the Triassic and/or Jurassic (see Table 4) cannot be answered from the FT data alone.

With respect to the Mesozoic temperature history, apatite FT modelling in general indicates high temperatures for most of the samples, supporting Triassic/Jurassic reheating. Modelling of the partially reset sample 229 confirms this. However, the question whether reburial or elevated geothermal gradients have caused the elevated temperature in this and other samples (34, 35 and 36) is difficult to resolve and if it were to resolve, probably would require a much larger number of fission track samples. However, it seems geologically reasonable not to exclude Triassic/Jurassic sedimentation. Sedimentary relics of this stratigraphic age are preserved on the opposite bank of the Rhine River, in the Eifel Depression to the south, and in the Central and Northern Ruhr Basin (e.g. at the locations of wells I3 and "H", Fig. 1). The fission-track results, and in particular those of samples 229, 34, 35 and 36, thus make it likely that Mesozoic sediments have transgressed over the northern and western rims of the Rhenish massif. Those sediments might have been deposited within a south to north elongated and fault-bounded accumulation space, as was already postulated by Murawski et al. (1983).

A similar Mesozoic thermal history pattern, derived from apatite fission-track data was reported from Büker (1996) at the eastern rim of the Rhenish massif. These data indicate elevated Mesozoic temperatures reached their maximum during the Jurassic. In analogy to the fission-track analysis results obtained from this study, this is interpreted as reheating related to the subsidence of the Hessian Depression, forming the eastern border of the Rhenish massif. In this area, thicknesses of eroded Triassic/Jurassic deposits remain speculative, but will probably not have exceeded a few hundred metres. It is therefore difficult to explain the average Mesozoic temperatures obtained from fission-track modelling only by subsidence, even if it is considered that a significant pile of Palaeozoic rocks might still have covered the samples during the Jurassic.

With respect to the question, whether samples have experienced reheating or reburial during the Triassic/Jurassic, it is interesting to compare these new results with earlier published FT age data. The similarity of the data presented in this study (136 ± 7 and 257 ± 13 Ma, except samples 46 and 229) to the data published by Glasmacher et al. (1998) for the western Rhenish massif (130 ± 22 and 239 ± 26 Ma) has already been pointed out. Nearly identical ages between 146 ± 15 Ma and 209 ± 13 Ma were obtained by Vercoutere and van den Haute (1993) in the Brabant massif of Belgium. Vercoutere and van den Haute (1993) assign these ages to thermal processes related to North Sea rifting and the opening of the North Atlantic. In this context, it is noteworthy that many post-Variscan hydrothermal ore deposits are found in the European Variscides ranging in age from 200 Ma to 130 Ma (Hagedorn 1992; Lüders et al. 1993; Jenkin et al. 1994; O'Reilly et al. 1997), which probably accounts for a regional or fault-related thermal perturbation of the Variscan crust at this time.

One important observation of this study is that the majority of fission-tracks in apatite have been significantly shortened in the partial annealing zone; i.e. the host rocks have remained at temperatures between 60°C and 120°C for a long period (see detailed discussions of samples in the previous paragraphs). The moderate to low Mesozoic and early Tertiary cooling rates (Table 4), as predicted from modelling FT data, imply that epirogenetic rather than rapid tectonic movements or thermal events caused erosion and cooling during this period. For Oligocene to Recent times, regional erosional cooling is probably linked to the development of the nearby Rhine Graben (Utescher et al. 2002). Continuous fall in regional base level with subsidence of the lower Rhine Basin could have triggered accelerated denudation and sediment discharge from the adjacent Rhenish massif.

A possible alternative cooling history, with cooling at a constant rate from the Permian or Triassic, when samples were cooled below 120°C, until recent time, when samples were exposed at the surface, would imply

that samples left the apatite FT partial annealing zone some 100–150 Ma before present. This would require that a high percentage of fission-tracks were not shortened and is not consistent with our observations.

Conclusions

- Apatite fission-track ages range from 291 ± 15 Ma to136 ± 7 Ma and are much younger than depositional ages for all samples from the Ruhr Basin and the northern Rhenish massif. This observation indicates that the Carboniferous and Devonian rocks were heated to temperatures sufficient to totally anneal apatite fission-tracks at temperatures above 120°C and is in accordance with the moderate to high levels of thermal maturity of the rocks.
- Exceptions to this trend are represented by samples 229 and 46, where some apatite grains with central ages older than the stratigraphic age, are observed. Thus, thermal resetting during late Palaeozoic times was incomplete. Sample 47 remained within the PAZ until present-day.
- Quantitative modelling of the apatite fission-track data predicts that samples from the Ruhr Basin experienced cooling from maximum temperatures during the latest Carboniferous/earliest Permian. Thereafter, temperatures remained below the temperature of total apatite fission-track annealing (< 120°C).
- For the Rhenish massif modelled apatite fission-track data indicate significant Variscan denudation, caused by major rock uplift. This most likely occurred during the Namurian or Westfalian. The results imply that sedimentation in the Rhenish massif, where late to early Devonian rocks crop out at present, lasted until the late Carboniferous. Future palaeogeographic maps should consider this.
- Apatite fission-track modelling indicates that some samples from both the Ruhr Basin and the Rhenish massif remained in the apatite partial annealing zone for a significant time. This may be explained by several hundred metres of now eroded sedimentary rocks or elevated heat flow during the Triassic/early Jurassic.
- The Mesozoic thermal history reconstructed, in this study, fits into the regional context and confirms that Palaeozoic rocks of the Rhenohercynian Zone of central Europe (Belgian and German territories) remained at temperatures within the PAZ during most of the Mesozoic and that latest uplift and denudation did not start before upper Cretaceous times.
- High Mesozoic temperatures are supposed to correspond to Triassic–early Jurassic reburial subsidence and sedimentation as well as to a rise of the regional thermal regime due to crustal extension and basin forming processes affecting Central Europe at Mid-Jurassic times.
- Mesozoic cooling rates were low (< 1°C/Ma), regardless as to whether Triassic/Jurassic sedimentation is either assumed or not. Cooling rates were accelerated during the Tertiary and average at about 0.7°C/Ma.

Acknowledgements Financial support by the German Research Foundation (DFG) is gratefully acknowledged. This study was part of the DFG priority programme, "Simulation orogener Prozesse am Beispiel der Varisziden". We thank F. Hansen and K. Poddig for mineral separation and sample preparation for fission-track analysis. The comments of Dr. Stuart Thomson and an anonymous reviewer helped to improve the manuscript considerably.

References

Ahrendt H, Clauer N, Hunziker JC, Weber K (1983) Migration of folding and metamorphism in the Rheinisches Schiefergebirge deduced from K–Ar and Rb–Sr age determinations. In: Martin H, Eder FW (eds) Intracontinental fold belts: case studies in the Variscan belt of Europe and the Damara belt, Namibia. Springer, Berlin, Heidelberg, New York, pp 323–338

Barbarand J, Carter A, Wood I, Hurford AJ (2003b) Compositional and structural control of fission-track annealing in apatite. Chem Geol 198:77–106

Barbarand J, Carter A, Hurford T, Wood, I (2003a) Compositional and structural control of fission-track annealing in apatite. Chem Geol 198:107–137

Brix M (2002) Thermal history of Palaeozoic rocks in the Meuse Valley between Charleville-Méziéres and Namur assessed from zircon fission track data. Geol. Belgica Intern. Meeting, Aardk. Mededel., 2002, XX, 000-000: 1–3

Büker C (1996) Absenkungs-, Erosions- und Wärmeflussgeschichte des Ruhrbeckens und des Rechtsrheinischen Schiefergebirges. Diss Univ Bochum, 212 S

Büker C, Carpitella F, Littke R, Welte D-H (1996) Burial and thermal history of Carboniferous sediments in Well Floverich 2E-1 (Aachen-Erkelenz coal district, Germany). Zentralblatt für Geologie und Paläontologie, Teil I: Allgemeine, Angewandte, Regionale und Historische Geologie 11–12:1261–1273

Donelick RA, Ketcham RA, Carlson WD (1999) Variability of apatite fission-track annealing kinetics: II. Crystallographic orientation effects. Am Mineralogist 84:1224–1234

Drozdzewski G (1993) The Ruhr coal basin (Germany): structural evolution of an autochthonous foreland basin. Int J Geol 23:231–250

Fielitz W, Mansy JL (1999) Pre- and synorogenic burial metamorphism in the Ardenne and neighboring areas (Rhenohercynian zone, central European Variscides). Tectonophysics 309:227–256

Franke W (2000) The mid-European segment of the Variscides: tectonostratigraphic units, terrane boundaries and plate tectonic evolution. In: Franke W, Haak V, Oncken O, Tanner D (eds) Orogenic Processes: quantification and modelling in the Variscan Belt. The Geol Soc, London, pp 35–61

Galbraith RF, Laslett GM (1990) Statistical models for mixed fission-track ages. Nucl tracks radiat measure 21:459–470

Galbraith RF, Laslett GM (1993) Statistical models for mixed fission-track ages. Nucl tracks radiat measure 21:459–470

Gallagher K (1995) Evolving temperature histories from apatite fission-track data. Earth Planet Sci Lett 136:421–435

Garver J (2002) Metamictisation of natural zircon: accumulation versus thermal annealing of radioactivity-induced damage. Contrib Miner Petrol 143:756–757

Glasmacher U, Zentilli M, Grist AM (1998) Apatite fission-track thermochronology of paleozoic sandstones and the Hill-Intrusion, Northern Linksrheinisches Schiefergebirge, Germany. In: Van den Haute P, De Corte F (eds) Advances in fission-track geochronology Solid Earth Sciences Library vol 10. Kluwer, Dordrecht pp 151–172

Gleadow AJW, Duddy LR, Green PF, Lovering JF (1986) Confined fission-track lengts in apatite: a diagnostic tool for thermal history analysis. Contr Miner Petrol 94:405–415

Glennie KW (2001) Exploration activities in the Netherlands and North–West Europe since Groningen. Geol Mijnbouw 80:71–84

Green PF, Duddy IR, Laslett GM, Hegarty KA, Gleadow AJW, Lovering JF (1989) Thermal annealing of fission-tracks in apatite 4: quantitative modelling techniques and extension to geological timescales. Chem Geol (Isot Geosci Sect) 79:155–182

Hagedorn B (1992) (U + Th)/He-, K/Ar- und Rb/Sr-Chronologie von Hämatit und Adular hydrothermaler Lagerstätten des Harzes. Diss Univ Heidelberg

Harland et al (1989) A geologic time table. Camebridge University Press, London

Hertle M, Littke R (2000) Coalification pattern and thermal modelling of the Permo-Carboniferous Saar Basin (SW-Germany). Intern J Coal Geol 42:273–296

Hurford AJ (1990) Standardization of fission-track dating calibration: recommendation by the Fission-track Working Group of the I.U.G.S. Subcommission on Geochronology. Chem Geol (Isot Geosci Sect) 80:171–178

Hurford AJ, Green PF (1983) The zeta age calibration of fission-track dating. Isot Geosci 1:285–317

Jenkin GRT, Craw D, Fallick AE (1994) Stable isotopic and fluid inclusion evidence for meteoric fluid penetration into an active mountain belt; Alpine Schist, New Zealand. J Metamorphic Geol 12(4):429–444

Karg H (1998) Numerische Simulation der thermischen Geschichte, Subsidenz und Erosion des westlichen Rechtsrheinischen Schiefergebirges, des Ruhrbeckens und der Niederrheinischen Bucht. Berichte des Forschungszentrums Jülich 3618

Ketcham RA, Donelick WA, Carlson WD (1999) Variability of apatite fission-track annealing kinetics: III Extrapolation to geological time scales. Am Mineralogist 84:1235–1255

Kramm U, Buhl D, Chemychev IV (1985) Caledonian or Variscan Metamorphism in the Venn-Stavelot massif, Ardennes? Arguments from a K–Ar and Rb–Sr Study. N J Geol Paläont Abh 171:339–349

Laslett GM, Galbraith RF (1996) Statistical modelling of thermal annealing of fission-tracks in apatite. Geochim Cosmochim Acta 60:5117–5131

Littke R, Büker C, Lueckge A, Sachsenhofer RF, Welte DH (1994) A new evaluation of palaeo-heat flows and eroded thicknesses for the Carboniferous Ruhr basin, western Germany. Int J Geol 26(3–4):155–183

Littke R, Büker C, Hertle M, Karg H, Stroetmann-Heinen V, Oncken O (2000) Heat flow evolution, subsidence and erosion in the Rheno-Hercynian ororgenic wedge of central Europe. In: Franke W, Haak V, Oncken O, Tanner D (eds) Orogenic Processes: Quantification and Modelling in the Variscan Belt. Geol Soc Lond Spec Publ 179:231–255

Lommerzheim AJ (1994) Die Genese und Migration der Erdgase im Muensterlaender Becken (Formation and migration of natural gas in the Münsterland Basin). Fortschritte in der Geologie von Rheinland und Westfalen 38:308–348

Lüders V, Gerler J, Hein UF, Reutel C (1993) Chemical and thermal development of ore-forming solutions in the Harz Mountains: A summary of fluid inclusion studies. In: Möller P, Lüders V (eds) Formation of of hydrothermal vein deposits—a case study of the Pb–Zn, barite and fluorite deposits of the Harz Mountains. Monograph Series on Mineral Deposits, 30:117–132

McKerrow WS, MacNiocaill C, Ahlberg P, Clayton G, Cleal CJ, Eager RMC (2000) The late Palaeozoic relations between Gondwana and Laurussia. In: Franke W, Haak V, Oncken O, Tanner D (eds) Orogenic Processes: Quantification and Modelling in the Variscan belt. Geol Soc Spec Publ 179:9–20

Murawski H, Albers HJ, Bender P, Bremers HP, Dürr St, Huckriede R, Kauffmann G, Kowalczyk G, Meiburg P, Müller R, Ritzkowski S, Schwab K, Semmel A, Stapf K, Walter R, Winter KP, Zankl H (1983) Regional tectonic setting and geologic structure of the Rhenish massif. In: Plateu Uplift (eds Fuchs K, et al), pp 9–38

Naeser ND, Naeser CW, McCulloch TH (1989) The application of fission-track dating to the depositional and thermal history of rocks in sedimentary basins. In: Naeser ND, McCulloch TH (eds) Thermal histories of sedimentary basins—methods and case histories. Springer, New York, Berlin, Heidelberg, pp 157–180

Nöth S, Karg H, Littke R (2001) Reconstruction of late Paleozoic heat flows and burial histories at the Rhenohercynian-Subvariscan boundary, Germany. Int J Earth Sci 90(2):234–256

Oncken O (1989) Geometrie, Deformationsmechanismen und Kinematik grosser Störungszonen der hohen Kruste (Beispiele Rheinisches Schiefergebirge). Geotekton Forschungen 73:1–215

Oncken O (1991) Aspects of the structural and paleogeothermal evolution of the Rhenish massif. Ann Soc Geol Belg 113:139–159

O'Reilly, Jenkin GRT, Feely M (1997) A fluid inclusion and stable isotope study of 200 Ma of fluid evolution in the Galway Granite, Conemara, Ireland. Contrib Miner Petrol 129:120–142

Patteisky KE, Teichmüller M, Teichmüller R (1962) Das Inkohlungsbild des Steinkohlengebirges an Rhein und Ruhr, dargestellt im Niveau von Flöz Sonnenschein. Fortschr Geol Rheinl u Westf 3:687–700

Piqué A, Huon S, Clauer N (1984) La schistosité hercynienne et le metamorphisme associé dans la Valleé de la Meuse, entre Charleville-Mézières et Namur (Ardennes franco-belges). Bull Soc Belge Geol 93:70–77

Tait J, Schätz M, Bachtadse V, Soffel H (2000) Palaeomagnetism and Palaeozoic palaeogeography of Gondwana and European terranes. In: Franke W, Haak V, Oncken O, Tanner D (eds) Orogenic Processes: Quantification and Modelling in the Variscan belt. Geol Soc Spec Publ 179:21–34

Tschernoster R, Glasmacher U, Spaeth G, Clauer N (1995) K-Ar-Datierungen zur Abkühlungsgeschichte ausgewählter Magmatite und Metapelite aus dem Stavelot-Venn Massiv. In: Walter R, Glasmacher U, Wolf M (eds) KW-Relevante Eigenschaften potentieller Mutter- und Speichergesteine am Nordrand des Linksrheinischen Schiefergebirges IV:1–20

Utescher T, Mosbrugger V, Ashraf AR (2002) Facies and paleogeography of the Tertiary lower Rhine Basin—sedimentary versus climatic control. Neth J Geosci/Geol Mijnbouw 81(2):185–191

Vercoutere C, van den Haute P (1993) Post-Palaeozoic cooling uplift of the Brabant massif as revealed by apatite fission-track analysis. Geol Mag 130(5):639–646

Verweij JM, Simmelink HJ, van Balen RT, David P (2003) History of petroleum systems in the southern part of the Broad Fourteens Basin. Neth J Geosci 82(1):71–90

Walter R (1995) Geologie von Mitteleuropa. Schweitzerbart, Stuttgart, p 561